

High-activity catalyst of $\text{SO}_4^{2-}/\text{ZrO}_2$ supported on $\gamma\text{-Al}_2\text{O}_3$ for *n*-butane isomerization

T. Lei, J.S. Xu, W.M. Hua, Y. Tang and Z. Gao *

Department of Chemistry, Fudan University, Shanghai 200433, PR China

Received 29 April 1999; accepted 15 July 1999

A series of $\gamma\text{-Al}_2\text{O}_3$ -supported $\text{SO}_4^{2-}/\text{ZrO}_2$ superacid catalysts (named SZ/ Al_2O_3) were prepared by a precipitation method and their catalytic behavior for *n*-butane isomerization at low temperature in the absence of H_2 and at high temperature in the presence of H_2 was studied in this paper. The catalytic activities of some of these catalysts were enhanced significantly at both low and high temperatures. At 250 °C after 6 h on stream, the steady activity of the most active sample, 60%SZ/ Al_2O_3 , is about two times higher than that of conventional SZ. The texture properties of catalysts were studied by the methods of XRD and the adsorption of N_2 . Experimental evidence of IR of adsorbed pyridine indicates that the significant activity enhancements of SZ/ Al_2O_3 catalysts are caused by the increasing of the amount of strong acid sites.

Keywords: *n*-butane isomerization, sulfated zirconia, SZ/ Al_2O_3 , $\gamma\text{-Al}_2\text{O}_3$ carrier

1. Introduction

The isomerization of *n*-butane to isobutane, which is a valuable precursor for the production of MTBE and alkylated gasoline, is an important process in refining industry. Strong solid acids, especially sulfated zirconia, have been found to be very active for *n*-butane isomerization at comparatively lower temperatures [1]. Many researchers [2–10] were attracted by sulfated zirconia due to its high catalytic activity and its being surrounding friendly.

However, from a practical point of view, there are still some problems to be solved. On the one hand, the activity and stability of the SZ catalyst must be further improved. On the other hand, it seems difficult to use sulfated zirconia as a commercial catalyst, because the conventional preparation method of hydrolyzing zirconium salt [2,3] results in high cost and the particles of unsupported sulfated metal oxides are generally very small, which makes operation difficult [11]. In order to solve these problems, one of the good methods is supporting SZ on a suitable carrier. Yamaguchi et al. [11] have studied the dispersion behavior of $\text{SO}_4^{2-}/\text{Fe}_2\text{O}_3$ on SiO_2 support. Huang et al. [12] have supported the sulfated titania on silica and studied its activity for cumene cracking reaction. Sulfated zirconia has been supported on silica by Ishida et al. [13], and its activity for the ring-opening isomerization of cyclopropane has been studied. Only a few papers [14] are reported on supporting sulfated zirconia on a $\gamma\text{-Al}_2\text{O}_3$ carrier, but no literature about using it as *n*-butane isomerization catalyst is known to the present authors.

In this work, we prepared a series of $\gamma\text{-Al}_2\text{O}_3$ -supported SZ catalysts, SZ/ Al_2O_3 , by a precipitation method. Their catalytic activities for *n*-butane isomerization were studied

both at low and high temperatures. Information about the structure of these catalysts was obtained by the methods of XRD and the adsorption of N_2 . The acid strength and the amount of acid sites of the catalysts were characterized by *n*-butane isomerization at 35 °C and IR techniques of adsorbed pyridine. The reasons for the improvement on catalytic activity of these supported strong acid catalysts in *n*-butane isomerization were discussed.

2. Experimental

A series of $\gamma\text{-Al}_2\text{O}_3$ -supported $\text{SO}_4^{2-}/\text{ZrO}_2$ catalysts (named SZ/ Al_2O_3) were prepared by a precipitation method. Appropriate amounts of zirconium nitrate were dissolved in water and $\gamma\text{-Al}_2\text{O}_3$ (Shanghai Chemical Reagent Corporation, surface area 120 $\text{cm}^2 \text{g}^{-1}$) was then added to this aqueous solution in a suspended state. After hydrolysis by adding aqueous ammonia, the precipitate was filtered, washed and then dried at 110 °C for 6 h. The obtained material was immersed in 0.5 mol/l H_2SO_4 solution for 30 min and then dried at 110 °C. The final calcination temperature of the samples was 650 °C (or other designed temperatures). The SO_4/ZrO_2 catalyst (named SZ) was prepared by hydrolyzing $\text{ZrOCl}_2 \cdot 8\text{H}_2\text{O}$ with aqueous ammonia and then treating it with 0.5 mol/l H_2SO_4 . The final calcination temperature is also 650 °C. The detailed preparation method is described in the literature [15].

X-ray powder diffraction measurements were performed on a Rigaku D/MAX-IIA instrument with Cu $K\alpha$ radiation, scan speed 16°/min and scan range 20–70°. The data of BET surface areas and pore size distributions of the samples were acquired on a Micromeritics ASAP 2000 system under liquid- N_2 temperature using N_2 as the adsorbent. A chemical method was used for the detection of

* To whom correspondence should be addressed.

sulfur content in the catalysts. Dehydrated Na₂CO₃ and ZnO were used as fusing agents, and the sulfate was turned into BaSO₄ and determined by gravimetric method. The acidities of the samples were measured by the method of IR spectroscopy of pyridine adsorption. A self-supporting disk of the sample was evacuated at 400 °C for 2 h under a vacuum of 10⁻³–10⁻⁴ Pa. The pretreated catalyst, after the measurement of its IR spectrum, was dosed with an excess of pure pyridine vapor. IR spectra of the chemisorbed pyridine were recorded after evacuation at desired temperatures. Lewis acidities were determined on the basis of the absorbances of the Py L band near 1444 cm⁻¹. Infrared spectra of the samples were recorded on a Perkin–Elmer 983G infrared spectrometer. The coke deposit on the catalysts was detected on a Carlo–Erba 1106 elemental analysis instrument.

The isomerization of *n*-butane was performed both at low and high temperatures. At 35 °C a closed reaction system was used. 0.5 g catalyst was placed in a glass cell, and 5 ml (STP) of *n*-butane of 99.9% purity was injected for each test. The reaction at 250 °C was carried out in a flow-type fixed-bed reactor under ambient pressure. 1.0 g catalyst was loaded, and a mixture of butane and H₂ (1 : 10 molar ratio) was fed at a rate of WHSV 0.3 h⁻¹. The catalysts were preheated *in situ* in dry air at 450 °C for 3 h. The reaction products were analyzed by a gas chromatograph equipped with FID. The used catalysts were regenerated by calcination *in situ* in dry air at 450 °C for 3 h.

3. Results and discussion

3.1. Catalyst characterization

XRD patterns of SZ and SZ/Al₂O₃ samples with different ZrO₂ contents are depicted in figure 1. After calcination at 650 °C, a portion of the monoclinic phase is present in SZ along with the tetragonal phase. For the SZ/Al₂O₃ samples, however, only the tetragonal phase appears and the intensities of the tetragonal peak increase with the increasing of zirconia content from 15 to 90 wt%. XRD patterns of the 60%SZ/Al₂O₃ sample calcined at different temperatures are depicted in figure 2. The tetragonal phase persists alone in these samples and the monoclinic phase does not appear even after calcination at 750 °C. From the results above, it is clear that the transformation from the metastable tetragonal phase to the monoclinic phase is retarded. In other words, the tetragonal phase of zirconia is stabilized after being supported on a γ -Al₂O₃ carrier. This phenomenon was also observed by Grau et al. [14] and they attributed it to the strong interaction between zirconia and carrier. In addition, as shown in figure 1, the characteristic peaks of the γ -Al₂O₃ carrier ($2\theta = 45.7$ and 66.7°) were observed only at low zirconia content (15–30 wt%), but they disappear when the zirconia content is further increased. According to the literature [16], this may be due to the presence of interaction between zirconia and alumina or the covering of the alumina support by ZrO₂ crystallites.

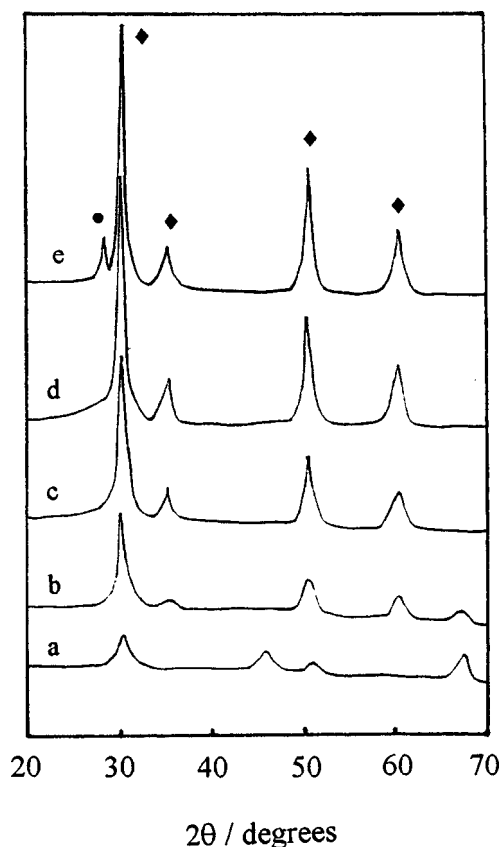


Figure 1. XRD patterns of SZ/Al₂O₃ samples calcined at 650 °C: (a) 15%SZ/Al₂O₃, (b) 30%SZ/Al₂O₃, (c) 60%SZ/Al₂O₃, (d) 90%SZ/Al₂O₃, (e) SZ.

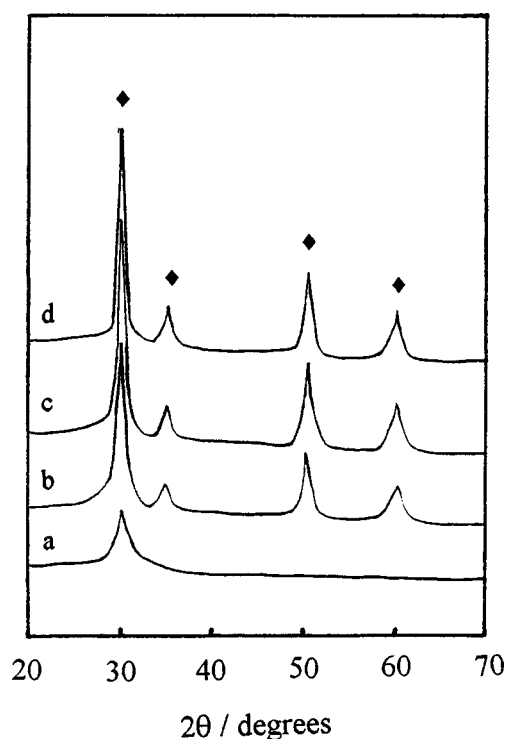


Figure 2. XRD patterns of 60%SZ/Al₂O₃ samples calcined at different temperatures: (a) 550 °C, (b) 600 °C, (c) 700 °C, (d) 750 °C.

The surface area, pore volume and sulfur content of the catalysts are listed in table 1. Although the BET surface areas of the SZ and SZ/Al₂O₃ samples are comparable, the total pore volume of the catalysts decreases gradually with the increasing of the ZrO₂ content. When zirconia content approaches to 100% (pure SZ), the pore volume of the sample is only 0.09 cm³/g. The pore size distribution curves of the SZ/Al₂O₃ samples are illustrated in figure 3. As shown, the large pore of γ -Al₂O₃ decreases with the increasing of the zirconia content and its centered pore size shifts to low value. This result indicates that the large pores of γ -Al₂O₃ carriers are blocked by small zirconia crystallites, which results in the decreasing of the pore volume.

The sulfur contents of the SZ/Al₂O₃ series catalysts are much higher, as shown in table 1. Comparing to SZ, they increase by about 20–40%. It seems that the addition of γ -Al₂O₃ as a carrier may help to stabilize the surface sulfate complexes remarkably. The similar phenomenon was also observed by Grau et al. [14].

Table 1
Surface area, pore volume and SO₃ content of various samples after calcination at 650 °C.

Sample	Surface area (m ² /g)	Pore volume (cm ³ /g)	SO ₃ content (wt%)
15%SZ/Al ₂ O ₃	120.9	0.53	4.5
30%SZ/Al ₂ O ₃	128.5	0.43	4.6
60%SZ/Al ₂ O ₃	133.5	0.30	4.3
90%SZ/Al ₂ O ₃	106.3	0.15	4.0
SZ	113.0	0.09	3.3

3.2. Acid properties

Infrared spectra of the catalysts after evacuation at 400 °C for 2 h display a strong band at about 1390 cm⁻¹, which is characteristic of the surface sulfate species with covalent S=O bonds [17]. When pyridine is adsorbed on the catalyst surface, a drastic shift of this IR band is observed. According to the literature [17], this red shift of the 1390 cm⁻¹ band indicates a strong interaction between the adsorbed pyridine molecule and the surface sulfur complex. The frequency shift corresponding to a decrease in the bond order of the S=O covalent bond and an increase in the partial charge on the oxygen atom are associated with the acid strength of the catalyst. Table 2 lists the data of S=O stretching frequency, bond order and partial charge on oxygen for the catalysts. The data of bond order and partial charge on oxygen before and after pyridine adsorption were calculated according to equations given in the literature [17,18]. It is clear that the frequency shift of the S=O covalent bond of 60%SZ/Al₂O₃ is almost identical with that of SZ, indicating that their acid strengths are comparable.

The infrared spectra of pyridine adsorbed on samples in the spectral region 1700–1300 cm⁻¹ give information about the type of acid sites and acid strength distribution present in the samples. After adsorbing pyridine, the absorption bands at 1608 and 1444 cm⁻¹ of pyridine were observed in the infrared spectra of the SZ and 60%SZ/Al₂O₃ samples, but the absorption band at 1540 cm⁻¹ does not appear. It indicates that there are only Lewis sites on the surface of the samples but no Brønsted sites. Morterra et al. [19] also

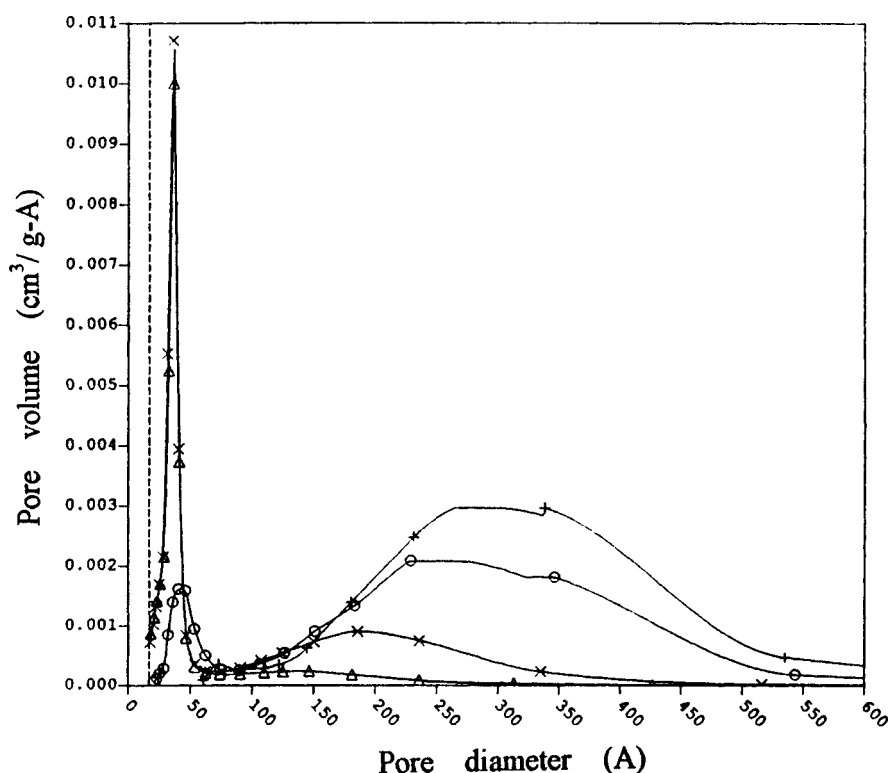


Figure 3. Pore size distributions of samples: (+) SO₄²⁻/γ-Al₂O₃, (○) 15%SZ/Al₂O₃, (×) 60%SZ/Al₂O₃, (Δ) 90%SZ/Al₂O₃.

Table 2
Stretching frequency, bond order and partial charge on oxygen of S=O before and after pyridine adsorption.^a

Sample	SO stretching frequency (cm ⁻¹)			Bond order		Partial charge on oxygen	
	B	A	Shift	B	A	B	A
SO ₄ ²⁻ /ZrO ₂	1390	1334	56	1.86	1.77	-0.14	-0.23
60%SZ/Al ₂ O ₃	1397	1338	59	1.87	1.78	-0.13	-0.22

^a B: before pyridine adsorption; A: after pyridine adsorption. The pyridine desorption temperature is 150 °C.

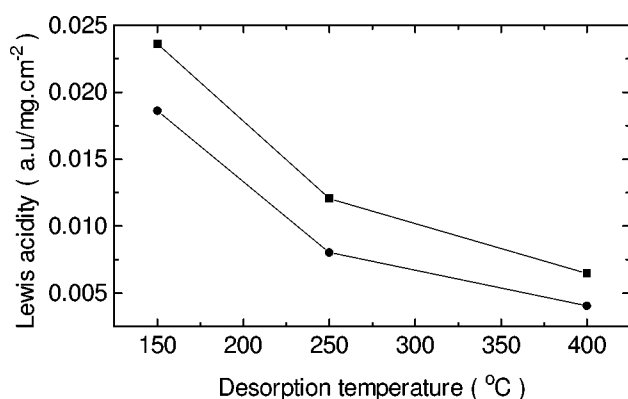


Figure 4. Amount of L acidity at different desorption temperatures: (■) 60%SZ/Al₂O₃, (●) SZ.

observed this phenomenon and attributed it to the dehydration after desorption at 400 °C under vacuum treatment condition. In order to study the acid strength distribution on the samples, the variations of the 1444 cm⁻¹ band intensities of the pyridine species as a function of outgassing temperature were investigated and the results are depicted in figure 4. As shown, the amount of Lewis acid sites of the 60%SZ/Al₂O₃ sample is higher than that of SZ after desorption at both 150 and 400 °C. According to the literature [20], in an experiment of microcalorimetric measurement, the acid sites with heats of ammonia adsorption more than 125 kJ/mol correspond to the acid sites with pyridine molecules irreversibly adsorbed at 350 °C. It is reasonable to assume that the amount of acid sites measured after desorption at 150 °C represents the total acid sites of the catalyst and that measured after desorption at 400 °C corresponds to the strong acid sites. So, it is clear that the amounts of both total acid sites and strong acid sites of 60%SZ/Al₂O₃ are higher than those of SZ.

3.3. Isomerization reaction

The kinetics of *n*-butane isomerization on strong solid acid catalysts at low temperature obeys the rate law of a first-order reversible reaction, and the isomerization activity correlates fairly well with strong acidity of the catalysts. Therefore, the isomerization of *n*-butane at 35 °C can be used as a probe reaction to measure strong acidity of catalysts [21]. Figure 5 depicts the relationship between ZrO₂ content of the SZ/Al₂O₃ catalysts and *n*-butane isomerization activity at 35 °C. The catalytic activity (or strong acidity) is represented by the forward rate constant *k*₁. It can be seen that the isomerization activity of the SZ/Al₂O₃

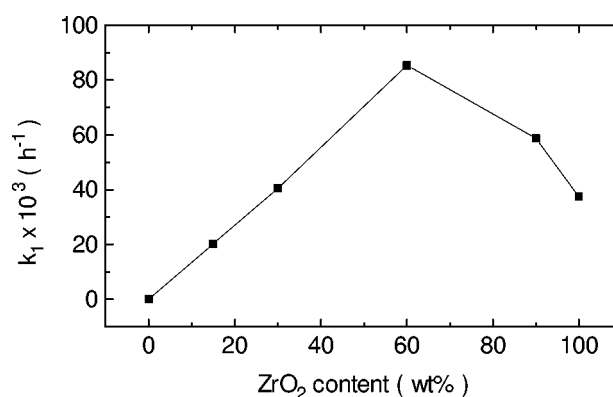


Figure 5. Relationship between ZrO₂ content of SZ/Al₂O₃ catalysts (all catalysts were calcined at 650 °C) and *n*-butane isomerization activity at 35 °C.

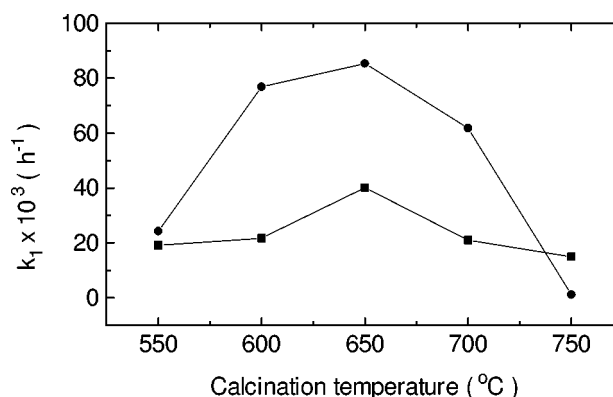


Figure 6. Relationship between calcination temperature and *n*-butane isomerization activity at 35 °C: (●) 60%SZ/Al₂O₃, (■) SZ.

catalysts increases rapidly with increasing of the ZrO₂ content up to 60%, and then decreases as the ZrO₂ content is further increased. The 60%SZ/Al₂O₃ sample has the highest acidity and its *k*₁ value is about two times greater than that of SZ. The effect of the calcination temperature on the strong acidities of the samples is depicted in figure 6. As illustrated, the strong acidity of 60%SZ/Al₂O₃ is higher than that of SZ at all range of calcination temperatures except at 750 °C. The optimum calcination temperature for the 60%SZ/Al₂O₃ catalyst is 650 °C and it is identical with that for the SZ catalyst. The results of figures 5 and 6 indicate that the strong acidity of the SZ catalyst could be improved significantly by being supported on a γ -Al₂O₃ carrier under appropriate preparation conditions. This improvement effect can be explained by the results of XRD and IR measurement of adsorbed pyridine. Many papers have reported

that the tetragonal phase is the active phase [22,23] and the transformation from the metastable tetragonal phase to the monoclinic phase is related to the deterioration of the strong acidity of the sample [7,24]. In the case of SZ/Al₂O₃ series catalysts, the tetragonal phase of zirconia is stabilized and the transformation from tetragonal to monoclinic is delayed. Furthermore, from the results of IR measurement of adsorbed pyridine, it was found that the highly active SZ/Al₂O₃ catalysts, for instance 60%SZ/Al₂O₃, have larger amount of strong acid sites which may result in the improving of catalytic activities.

The major reaction product of *n*-butane isomerization at 250 °C is isobutane, and the steady selectivities to isobutane for all the catalysts are above 90%. The variations of the conversion of *n*-butane isomerization at 250 °C with time on stream for SZ/Al₂O₃ and SZ catalysts calcined at 650 °C are given in table 3. As shown, the initial activities of the samples increase with the contents of zirconia up to 60% and then decrease slowly with further increasing of the zirconia content. This variation rule is in agreement with the strong acidity of the catalysts measured by *n*-butane isomerization at low temperature. The above results indicate that the enhancement in activity of SZ/Al₂O₃ series catalysts for the *n*-butane isomerization at 250 °C in the presence of H₂ is caused by an increase in the amount of strong acid sites. Although the SZ/Al₂O₃ series catalysts deactivate more rapidly than SZ during the first 2 h of the reaction (see table 3), from then on the conversion of some of the former catalysts (60%SZ/Al₂O₃ and 90%SZ/Al₂O₃) drops very little, while that of the SZ catalyst still drops obviously. After 6 h on stream, the steady activities of the 60%SZ/Al₂O₃ and 90%SZ/Al₂O₃ catalysts are about two times higher than that of the SZ catalyst.

Table 3
Activity for *n*-butane isomerization at 250 °C in flow system.

Sample	Conversion (%)					
	2 min	10 min	60 min	120 min	180 min	360 min
15%SZ/Al ₂ O ₃	13.9	11.7	4.6	2.6	1.8	0.8
30%SZ/Al ₂ O ₃	33.2	31.6	26.3	21.6	18.0	14.7
60%SZ/Al ₂ O ₃	53.9	48.2	39.7	38.7	38.3	38.3
90%SZ/Al ₂ O ₃	53.4	43.4	39.5	38.7	38.5	38.1
SZ	27.7	25.2	24.5	21.6	20.4	18.5

From the view point of practical use in industry, because the 60%SZ/Al₂O₃ catalyst has the feature of lower cost besides its high activity and stability, it can be considered as a good candidate for commercial-scale *n*-butane isomerization catalyst.

The coke deposited on the catalysts after reaction was analyzed. The results are given in table 4. Although the amount of coke deposited on the SZ/Al₂O₃ catalysts after being on stream for 6 h is higher than that on SZ, the steady activities of 60%SZ/Al₂O₃ and 90%SZ/Al₂O₃ are much higher than that of SZ, implying that the amount of active acid sites left on the former may be higher than that on the latter.

The regeneration ability of a catalyst is very important in the practical use in industry. As illustrated in figure 7, the 60%SZ/Al₂O₃ catalyst has excellent regeneration ability. After a regeneration process of heating the used catalyst *in situ* in dry air at 450 °C for 3 h, the activity of the refreshed catalyst is almost identical with that of the fresh catalyst. The sulfur content of catalysts after reaction 6 h on stream is given in table 4. As shown in tables 1 and 4, the SO₃ content of used catalysts is a bit lower than that of fresh catalysts, implying that very little amount of sulfur was removed from the catalysts. Some authors suggested that the deactivation of the SZ catalyst is due to the loss of sulfur [25], while others considered that the formation of coke on the catalyst surface caused the drop in catalytic activity [6,26,27]. Since the deactivated catalyst can be completely regenerated by burning off the coke in air, we feel confident to propose that coke formation is the main reason for the deactivation.

Table 4
Coke and sulfur contents of used catalysts.^a

Catalyst	Coke (wt%)	SO ₃ content (wt%)
15%SZ/Al ₂ O ₃	1.29	4.2
30%SZ/Al ₂ O ₃	1.16	4.4
60%SZ/Al ₂ O ₃	1.31	4.0
90%SZ/Al ₂ O ₃	1.36	3.9
SZ	0.42	3.1

^a After reaction on stream for 6 h.

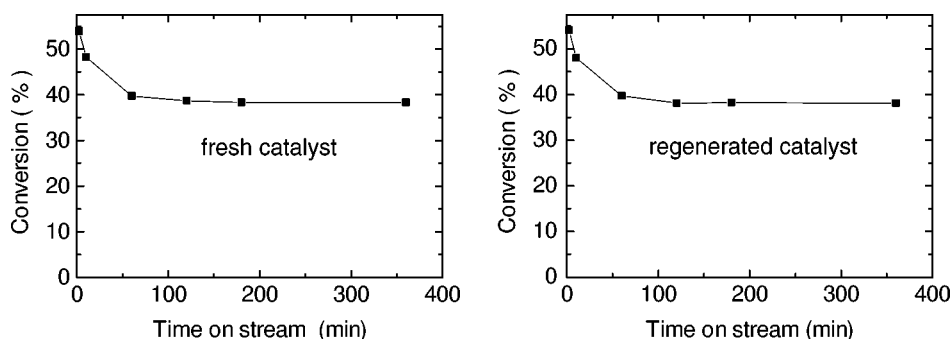


Figure 7. Regeneration ability of 60%SZ/Al₂O₃ catalyst.

4. Conclusions

Supporting strong solid acid SZ on γ -Al₂O₃ is a good way to obtain a highly active and stable catalyst for *n*-butane isomerization. The introduction of γ -Al₂O₃ as a carrier retards the phase transformation of ZrO₂ from tetragonal to monoclinic and helps to stabilize the sulfur species on the surface of the catalyst. More important, after supporting SZ on γ -Al₂O₃, the amount of strong Lewis sites on the catalyst surface increases greatly, which results in an increase in *n*-butane isomerization activity. The steady activity of the most active catalyst, 60%SZ/Al₂O₃, is about two times higher than that of the conventional SZ. Considering its high activity and low cost, 60%SZ/Al₂O₃ can be considered as an excellent practical catalyst candidate for *n*-butane isomerization.

References

- [1] K. Arata and M. Hino, *Mater. Chem. Phys.* 26 (1990) 213.
- [2] M. Hino, S. Kobayashi and K. Arata, *J. Am. Chem. Soc.* 101 (1979) 6439.
- [3] M. Hino and K. Arata, *J. Chem. Soc. Chem. Commun.* (1980) 851.
- [4] H. Matsuhashi, M. Hino and K. Arata, *Chem. Lett.* (1988) 1027.
- [5] J.C. Yori, J.C. Luy and J.M. Parera, *Appl. Catal. A* 46 (1989) 103.
- [6] F.R. Chen, G. Coudurier, J.-F. Joly and J.C. Vedrine, *J. Catal.* 143 (1993) 616.
- [7] J.H. Lunsford, H. Sang, S.M. Campbell, C.H. Liang and R.G. Anthony, *Catal. Lett.* 27 (1994) 305.
- [8] Z. Gao, J.M. Chen, W.M. Hua and Y. Tang, *Stud. Surf. Sci. Catal.* 90 (1994) 507.
- [9] C. Morterra, G. Cerrato, F. Pinna, M. Signoretto and G. Strukul, *J. Catal.* 149 (1994) 181.
- [10] H. Liu, G.D. Lei and W.M.H. Sachtler, *Appl. Catal. A* 146 (1996) 165.
- [11] T. Yamaguchi, T. Jin, T. Ishida and K. Tanabe, *Mater. Chem. Phys.* 17 (1987) 3.
- [12] Y.-y. Huang, B.-y. Zhao and Y.-c. Xie, *Appl. Catal.* 171 (1998) 65.
- [13] T. Ishida, T. Yamaguchi and K. Tanabe, *Chem. Lett.* (1988) 1869.
- [14] J.M. Grau, C.R. Vera and J.M. Parera, *Appl. Catal. A* 172 (1998) 311.
- [15] C.X. Miao and Z. Gao, *Mater. Chem. Phys.* 50 (1997) 15.
- [16] S. Damyanova, P. Grange and B. Delmon, *J. Catal.* 168 (1997) 421.
- [17] T. Jiu, T. Yamaguchi and K. Tanabe, *J. Phys. Chem.* 90 (1986) 4794.
- [18] R.J. Gillespie and E.A. Robinson, *Canad. J. Chem.* 41 (1963) 2074.
- [19] C. Morterra, R. Aschieri and M. Volante, *Mater. Chem. Phys.* 20 (1988) 539.
- [20] K. Shimizu, N. Kounami, H. Wada, T. Shishido and H. Hattori, *Catal. Lett.* 54 (1998) 153.
- [21] Z. Gao, J.M. Chen, W.M. Hua and Y. Tang, *Acid-Base Catalysis II* (Kodansha, Tokyo, 1994) p. 507.
- [22] C. Morterra, G. Cerrato, F. Pinna and M. Signoretto, *J. Catal.* 157 (1995) 109.
- [23] R.A. Comelli, C.R. Vera and J.M. Parera, *J. Catal.* 151 (1995) 96.
- [24] T. Yamaguchi and K. Tanabe, *Mater. Chem. Phys.* 16 (1986) 67.
- [25] F.T.T. Ng and N. Haovat, *Appl. Catal. A* 123 (1995) L197.
- [26] P. Nascimento, C. Akrapoulou, M. Oszagyan, G. Coudurier, C. Travers, J.F. Joly and J.C. Vedrine, *Stud. Surf. Sci. Catal.* 75 (1993) 1197.
- [27] B.H. Li and R.D. Gonzalez, *Appl. Catal. A* 174 (1998) 109.